Integrative Biology

RSC Publishing

PAPER

View Article Online
View Journal | View Issue

Published on 27 March 2013. Downloaded by University of Arizona on 29/09/2014 15:24:34.

Cite this: *Integr. Biol.*, 2013, **5**, 807

Hormonally responsive breast cancer cells in a microfluidic co-culture model as a sensor of microenvironmental activity†

Jessica D. Lang,[ab] Scott M. Berry,[ac] Ginny L. Powers,[ab] David J. Beebe[ac] and Elaine T. Alarid*[ab]

Received 7th November 2012,
Accepted 26th March 2013

DOI: 10.1039/c3ib20265h

www.rsc.org/ibiology

Breast cancer cell growth and therapeutic response are manipulated extrinsically by microenvironment signals. Despite recognition of the importance of the microenvironment in a variety of tumor processes, predictive measures that incorporate the activity of the surrounding cellular environment are lacking. In contrast, tumor cell biomarkers are well established in the clinic. Expression of Estrogen Receptor-alpha (ERα) is the primary defining feature of hormonally responsive tumors and is the molecular target of therapy in the most commonly diagnosed molecular subtype of breast cancer. While a number of soluble factors have been implicated in ERα activation, the complexity of signaling between the cellular microenvironment and the cancer cell implies multivariate control. The cumulative impact of the microenvironment signaling, which we define as microenvironmental activity, is more difficult to predict than the sum of its parts. Here we tested the impact of an array of microenvironments on ERα signaling utilizing a microfluidic co-culture model. Quantitative immunofluorescence was employed to assess changes in ERα protein levels, combined with gene expression and phosphorylation status, as measures of activation. Analysis of microenvironment-induced growth under the same conditions revealed a previously undescribed correlation between growth and ERα protein down-regulation. These data suggest an expanded utility for the tumor biomarker ERα, in which the combination of dynamic regulation of ERα protein and growth in a breast cancer biosensor cell become a read-out of the microenvironmental activity.

Insight, innovation, integration

The *biological insight* is the concept that a tumor biomarker can be used to predict the activity of the surrounding microenvironment. We show here that ERα protein dynamics, a component of the ERα activation mechanism, correlates with the growth-promoting activity in the context of a cellular microenvironment. Secondly, this study highlights the added value of using the dynamics of biomarkers to evaluate complex intercellular interactions like those encountered in tumors. The *innovation* is the application of microfluidics and immunofluorescence-based measurement techniques to test the effect of a panel of multivariate signaling systems on the dynamics of ERα in tumor cells. The *integration* of microfluidics and ERα dynamics in response to complex extracellular signaling enables prediction of environment's influence on growth.

Introduction

The microenvironment is a complex set of cellular, structural, and secreted components essential for homeostasis.[1] In cancer, this tightly controlled environment is often altered in parallel or directly by the tumor,[2–4] resulting in changes in the regulation of processes such as proliferation,[5,6] cell survival,[7,8] and metastasis.[9,10] Breast cancer cell growth is clearly modulated by cellular microenvironment components, especially fibroblasts.[11,12] Decades of research on the microenvironment's role in breast cancer have sought to identify candidate factors that stimulate tumor growth. Yet cumulatively, these studies highlight that multiple extracellular signals have redundant effects on a number of tumor processes, presenting significant challenges for developing new therapies. Candidate factors, such as Epidermal Growth Factor,[13–15] neuregulins,[16] and

[a] *University of Wisconsin-Madison Carbone Comprehensive Cancer Center, Madison, WI 53705, USA*
[b] *Department of Oncology, University of Wisconsin-Madison, Madison, WI 53705, USA. E-mail: alarid@oncology.wisc.edu*
[c] *Department of Biomedical Engineering, University of Wisconsin-Madison, Madison, WI 53705, USA*

† Electronic supplementary information (ESI) available. See DOI: 10.1039/c3ib20265h

Published on 27 March 2013. Downloaded by University of Arizona on 29/09/2014 15:24:34.

Insulin-like Growth Factor-1,[17–19] have been identified using a number of approaches, from isolation from conditioned media to differential gene expression in tumors. However, the cumulative effects of biochemical properties of the extracellular environment on biological processes, or the microenvironmental activity, is challenging to understand and predict by examining the isolated effects of its parts. The complexity challenges the successful integration of measures of the microenvironment in the clinic, where biomarkers in the tumor cells are the gold standard. We postulated that biomarker dynamics in the breast cancer cells themselves might be used as a biosensor of the total microenvironmental activity. If correct, such an approach would be amenable to personalized medicine, as the patient's own biopsy samples could serve as the source of microenvironmental activity for screening.

Luminal breast cancers account for 50–80% of diagnosed breast cancer. These tumors are defined by their hormone-responsive profile, characterized by the expression of Estrogen Receptor-alpha (ERα), the primary therapeutic target in these breast cancers. The activity of this transcription factor is stimulated upon binding to its ligand, estrogen. Upon activation, the receptor targets a number of genes to either repress (ERα, *ESR1*[20,21]) or activate (Progesterone Receptor, *PGR*;[22,23] pS2, *TFF1*[24]) transcription. ERα protein levels decrease upon activation through both the down-regulation of its gene expression and proteolytic degradation of the receptor.[25] The full activity of ERα is dependent on Serine-118,[26] which is phosphorylated upon receptor activation.[27,28] ERα can also be activated in the absence of estrogen through such phosphorylation. Several extracellular factors have been implicated in estrogen-independent activity,[29–32] but the cumulative effect of multivariate microenvironment signaling components on ERα signaling is likely to be more complex. Selective ERα modulators (SERMs; *e.g.* Tamoxifen) and aromatase inhibitors (*e.g.* Anastrozole), are two major classes of hormone therapy used in the treatment of ERα-positive breast cancer, and target the estrogen-dependent but not the estrogen-independent activity. It is widely considered that the estrogen-independent activity of ERα underlies therapy resistance.

Cell culture models have been instrumental in the investigation of hormone responsive breast cancer and provide insight into therapy response. The MCF-7 cell line has been used extensively to model ERα-positive breast cancer both *in vitro* and in animal xenografts. Importantly, this cell model faithfully recapitulates estrogen-dependent growth and ERα activation and regulation seen *in vivo*. MCF-7 cells accurately model responses to hormone therapies observed in the clinic, making them an ideal candidate for a biosensor model, which integrates complex extracellular signals from a cellular microenvironment to identify changes in ERα signaling and proliferation.

Passive pumping microfluidics miniaturizes cell culture vessels to a volume on the order of microliters while maintaining operation using conventional lab supplies.[33] In traditional cell culture, large media volumes rapidly dilute secreted molecules. At the microscale, diffusion dominates the distribution of molecules in the media, and paracrine factors remain in close proximity to the cells, improving biological sensitivity[34] and control over the extracellular signaling environment.[35,36] The high-throughput capacity facilitates testing of complex mixtures of variables (multiple co-culture pairs, pharmacologic manipulation, screening, *etc.*) and increased numbers of replicates.[37] This enables direct comparisons within a panel of co-culture conditions in a single experiment, allowing side-by-side comparison of an array of microenvironment conditions.

Previously, the culture of small quantities of cells was limited by the availability of assays with sensitivity to detect and measure various biological endpoints. Detection of changes in protein levels is made possible by the quantification of immunofluorescence images acquired under appropriate conditions.[38,39] Additionally, image based quantification permits examination of protein distribution within a population using single-cell analysis techniques. Here we use quantitative immunofluorescence in an unbiased, microfluidic co-culture approach to measure the dynamics of ERα protein in the breast cancer cells under distinct mixtures of multivariate, extracellular signals from a diverse panel of cell lines representing. We demonstrate that decreases in ERα protein indicative of activation directly correlate with growth and therefore act as sensors for microenvironmental activity. This dynamic biomarker measurement defines subpopulations of microenvironments that could generate predictions on hormone therapy response.

Methods and materials

Cell lines and culture

Unless indicated otherwise, cells were maintained in media containing phenol red and L-glutamine supplemented with 10% fetal bovine serum (FBS; HyClone, Logan, UT, USA), 100 units per mL of penicillin, and 100 μg mL^{-1} streptomycin. Reagents were from Life Technologies (Carlsbad, CA, USA) if not indicated. MCF-7eGFP, HS-5, MDA-MB-231, MEF, MDA-MB-468, HS578T, HEK293, RMF/EG, and MRC-5 cells were cultured in high glucose DMEM (Mediatech, Inc., Herndon, VA, USA). THP-1, SK-BR-3, and T47D cells were cultured in RPMI 1640. CV-1 and BT-20 cells were cultured in MEM-alpha. MCF10A cells were cultured in DMEM/F12 containing 5% horse serum (Sigma-Aldrich, St. Louis, MO, USA) and supplemented with 20 ng mL^{-1} epidermal growth factor (Sigma-Aldrich), 500 ng mL^{-1} hydrocortisone (BD Biosciences, San Jose, CA, USA), and 10 μg mL^{-1} insulin (Sigma-Aldrich). MCF-7eGFP cells were generated by stable transfection of MCF-7 cells with the pEGFP-N1 and pBABEpuro plasmids using Lipofectamine 2000 according to the manufacturer's instructions, and selected with 1 μg mL^{-1} puromycin (Sigma-Aldrich).

Co-culture and hormone treatments

Prior to all experiments, cells were incubated in estrogen-deprived, phenol red-free media supplemented with 10% charcoal dextran stripped FBS, penicillin/streptomycin, and L-glutamine for 3 days and for the duration of the experiment. For quantitative real-time PCR (qRT-PCR) assays, MCF-7 cells were cultured alone or with HS-5 cells (2 : 1 ratio) at a total cell concentration of 4×10^5 cells per mL in a 6-well plate (2 mL total volume), and harvested after 24 hours for RNA isolation.

 This journal is © The Royal Society of Chemistry 2013

Published on 27 March 2013. Downloaded by University of Arizona on 29/09/2014 15:24:34.

For fluorescence growth assay, MCF-7eGFP cells were cultured alone or with various cell lines (2 : 1 ratio) at a total cell concentration of 3.3×10^4 cells per mL in a 96-well plate (150 μL total volume) and cultured for a period up to 5 days. For single microchannel assays, MCF-7eGFP cells were cultured alone or with various cell lines (2 : 1 ratio) at a total cell number of 1.6×10^4 cells per channel (4 μL total volume) for 24 hours. For compartmentalized microfluidic assays, 1.6×10^4 MCF-7 cells were cultured alongside 1.6×10^4 MCF-7 or HS-5 cells for 24 hours. Where hormone treatment is indicated, vehicle (0.1% ethanol; EtOH) or 17β-estradiol (E2; Steraloids, Inc., Newport, RI, USA) was added for the last 8 hours. In the macro-culture experiments, 10 nM E2 was used as a saturating dose. Microfluidic experiments were treated with an increased dose of 100 nM E2 to account for (1) polydimethyl siloxane (PDMS) adsorption of steroids from the media[40] and (2) non-saturating number of molecules in the smaller media volume per cell. This dose was determined to be the lowest dose at which a consistent estrogen response could be demonstrated in these devices. Treatments with 100 nM Tamoxifen (OHT; Sigma-Aldrich) and 10 nM to 10 μM Anastrozole (Ana; Sigma-Aldrich) were performed for the 24 hour duration of the co-culture.

Fluorescence growth assay

MCF-7eGFP cells were co-cultured with the cell line array (specific cell lines described in Fig. 1B) in triplicate in a white, opaque 96-well plate for 4 days. One day after seeding cells and each following day of culture, GFP fluorescence intensity was measured using a BioTek Synergy4 plate reader and Gen4 software (Winooski, VT, USA). Each day's measurement was normalized to its initial reading at day 1. The mean and standard deviation of the triplicate walls was calculated, and the Wilcoxon rank sum test was used to compare the means of three independent experiments using the Mstat program.[41]

qRT-PCR

Total RNA isolation, reverse transcription and qRT-PCR were performed as previously described.[42] E-cadherin mRNA (*CDH1*) served as a control for quantity of MCF-7 cells. Primer sequences are as follows: *ESR1* fwd 5′-CCTGATGATTGGTCTCGTCTG-3′ rev 5′-GGCACACAAACTCCTCTCC-3′; *PGR* fwd 5′-GCTGTCATTATGGTGTCCTTAC-3′ rev 5′-GTAGTTGTGCTGCCCTTCC-3′; *TFF1* fwd 5′-CGCCTTTGGAGCAGAGAG-3′ rev 5′-ACCACAATTCTGTCTTTCACG-3′; *CDH1* fwd 5′-TATTGAAAGAGAAACAGGATGG-3′ rev 5′-GGATGGTGTAAGCGATGG-3′. Relative RNA levels were calculated using the delta C_t method.[43] The Wilcoxon signed rank test was used to determine significance using the Mstat program.[44]

Microchannel fabrication

Microchannels were cast from polydimethyl siloxane (PDMS; Sylgard 184, Dow Corning, Midland, MI, USA) using traditional soft lithography methods. Briefly, relief molds were generated through selective exposure of a UV-curable epoxy (SU-8, Microchem, Newton, MA, USA) followed by development in propylene glycol. PDMS monomer was blended with hardener at 10 : 1 ratio, degassed for >30 minutes in a vacuum, poured onto the mold, and cured for >3 hours at 80 °C. Once cast, PDMS was peeled from the mold and bonded to pre-cleaned glass slides.

A

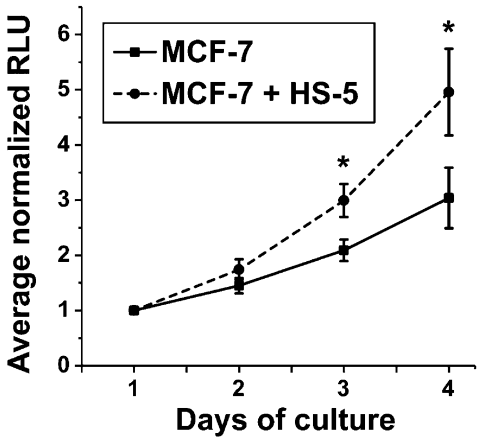

B

Co-cultured cell line	Cell line description	Fold change in growth at day 5	p-value
HS-5	*Homo sapiens* Bone marrow fibroblast	7.73	0.05
MDA-MB-231	*Homo sapiens* ERα-negative breast cancer epithelial	7.07	0.05
CV-1	*Cercopithecus aethiops* Normal kidney fibroblast	6.24	0.05
MCF10A	*Homo sapiens* ERα-negative breast epithelial	6.24	0.05
MEF	*Mus musculus* Embryonic fibroblast	5.92	0.05
MDA-MB-468	*Homo sapiens* ERα-negative breast cancer epithelial	5.60	0.05
HS-578T	*Homo sapiens* ERα-negative breast cancer epithelial	5.50	0.05
THP-1	*Homo sapiens* Acute monocytic leukemia monocyte	5.47	0.13
HEK293	*Homo sapiens* Embryonic kidney epithelial	4.75	0.51
SK-BR-3	*Homo sapiens* ERα-negative breast cancer epithelial	4.62	0.83
BT-20	*Homo sapiens* ERα-negative breast cancer epithelial	4.60	0.83
(mono)	MCF-7eGFP cells only	4.47	

Fig. 1 MCF-7eGFP cell growth in co-culture. MCF-7eGFP cells were directly co-cultured with various cell lines in steroid-free media in a 96-well plate. Fluorescence was first measured after 24 hours, and each day following to day 4. Each well's fluorescence was normalized to its day 1 value, and each condition was run in triplicate. (A) Initial co-culture of MCF-7eGFP cells with HS-5 cells and in mono-culture. Error bars represent standard deviation of 3 independent experiments. Statistical significance at each time point is represented by * ($p < 0.05$ *versus* mono-culture). (B) Summary of cell lines co-cultured in parallel with MCF-7eGFP cells. Fold change in growth represents mean fluorescence from MCF-7eGFP cells at day 5 relative to initial measurement. Statistical significance ($p < 0.05$) was determined after 3 independent experiments.

Published on 27 March 2013. Downloaded by University of Arizona on 29/09/2014 15:24:34.

PDMS–glass bonding was promoted by plasma treating in O_2 for 1 minute, contacting the PDMS and glass layers, then annealing at 135 °C for >2 minutes.

Immunofluorescence

Immunofluorescence staining was performed in single or compartmentalized microfluidic devices immediately following culture. Reagent addition and washes were performed with TBS (unless otherwise noted) by complete displacement of the original microchannel fluid content. Cells were fixed with 4% formaldehyde (Sigma-Aldrich) for 15 minutes, washed, permeablized for 30 minutes in 0.2% Triton X-100 (Sigma-Aldrich), then washed. A 10% goat serum (Sigma-Aldrich) solution in TBST was added for 1 hour for blocking, followed by addition of primary antibody in 5% goat serum in TBST overnight at 4 °C. Primary antibodies used are as follows: ERα 6F11 mouse monoclonal antibody, 1 : 200 (Vector Laboratories, Inc. Burlingame, CA, USA), ERα phospho-Serine-118 mouse monoclonal antibody, 1 : 200 (Cell Signaling, Danvers, MA, USA). Microchannels were washed with TBS, and Alexa Fluor 594 goat anti-mouse antibody in 5% goat serum in TBST was incubated for one hour. Following washing, 5 μg mL^{-1} Hoechst 33342 was added for 30 minutes, and channels were washed and stored in TBS until microscopy was performed.

Image acquisition

Images of immunofluorescence staining were acquired using a Nikon Eclipse Ti inverted fluorescence microscope and NIS Elements software. For each experiment, individual microchannels were scanned using each excitation filter to determine optimal exposure settings for each filter such that it neither saturated highest intensity staining nor failed to detect lowest intensity staining, thus allowing the most dynamic range of detection. Once settings were established, each channel was imaged for a field of view using 15× magnification on each of three filters (for Hoechst, GFP, and Alexa Fluor 594).

Image analysis

Images were analyzed using ImageJ software[45] (NIH, Bethesda, MD, USA). All images were opened simultaneously and compiled into a stack to ensure equivalent image processing. First, background subtraction was performed using a rolling ball filter to eliminate gradual pixel intensity changes throughout each image. The bottom 2% of pixels, which contribute to low background throughout the images, was eliminated by setting minimum pixel intensity to 5. The GFP images were then isolated to create GFP masks outlining MCF-7eGFP cell position. These masks were then used to remove non MCF-7 cell staining from nuclear and target protein (*i.e.* ERα) images. For population analysis, the integrated intensity of nuclear and target protein images were measured and analyzed in Excel by normalizing target protein intensity to nuclear intensity as a cell number correction. Fold changes of target protein expression were calculated relative to mono-culture controls. Within each experiment, 5–10 replicates were performed, and the Wilcoxon rank sum test was performed in Mstat for statistical significance. W test statistics were then combined from independent experiments to determine significance. For single-cell analysis, particle analysis was performed on nuclear images after GFP mask subtraction to define single nuclei and exclude overlapping nuclei. The regions of interest defining individual nuclei were redirected to the ERα protein images to measure signal intensity from individual nuclei. To generate a histogram, bins of ERα staining intensity were created, and frequency of nuclei in each bin was weighted for the total number of nuclei in each condition to generate a percentage of total nuclei per bin.

Fluorescence linearity determination

To determine the linear range of fluorescence intensity in image analysis, cells in single microchannels were substituted with 1.6×10^4 beads per mL InSpeck Green fluorescent microspheres (Molecular Probes, Eugene, OR, USA) with a diameter of 6 μm. These microspheres have known relative fluorescence intensities designed for generating calibration curves. Image acquisition and analysis were performed as described above.

Western blots

Western blots were performed using the Li-Cor Odyssey system, as per manufacturers instructions (Li-Cor, Lincoln, NE, USA). Blocking was performed in EMD Millipore Bløk-FL buffer (Billerica, MA, USA), which was also diluted 1 : 1 with TBS for use in all antibody incubations. Blots were incubated overnight with ERα H-184 rabbit polyclonal antibody (1 : 1000; Santa Cruz Biotechnology, Inc. Santa Cruz, CA, USA) and E-cadherin mouse monoclonal antibody (1 : 1000, BD Biosciences). IRDye 680CW anti-mouse and IRDye 800 anti-rabbit secondary antibodies (1 : 10 000; Li-Cor) were used after primary antibody incubation. A Li-Cor Odyssey infrared imager and software v3.0 were used to scan and quantify blots.

Results

Breast cancer cell growth in co-culture with an array of cell types

While enhanced cell growth is a defining property of cancer, the complete understanding of how the microenvironment influences growth has been technically challenging. Commonly used growth and proliferation assays, such as MTT assays and cell counting, cannot selectively measure a subpopulation of cells in a mixed culture. Assays that permit growth measurements in select cell subpopulations, such as flow cytometry, are complicated to scale to high-throughput analysis, necessitating miniaturization to the microscale. Stable expression of enhanced green fluorescent protein (eGFP) in the MCF-7eGFP cell line allows selective and technically simple growth measurement in a scalable assay. Fluorescence readings are proportional to the number of cells in a 96-well plate (Fig. S1, ESI†). To probe the microenvironmental activity of a model of bone metastasis, MCF-7eGFP cells were co-cultured directly with bone marrow stromal cell line, HS-5, in estrogen-free media for 5 days, and fluorescence was measured daily. HS-5 cells significantly stimulated the growth of MCF-7eGFP cells,

 This journal is © The Royal Society of Chemistry 2013

Published on 27 March 2013. Downloaded by University of Arizona on 29/09/2014 15:24:34.

detectable by the third day of culture (Fig. 1A). The HS-5 cell model serves as proof-of-principle that growth of hormonally responsive cells can be stimulated in a microenvironment model.

This assay was expanded to characterize a panel of diverse cell types in co-culture with MCF-7eGFP cells. The cell lines described in Fig. 1B were selected for the co-culture array to define patterns based on cell type and organ of origin in unbiased models of microenvironmental activity. Two non-human cell lines were included as further unbiased models of extracellular signaling in the induction of growth. The eleven cell lines were individually co-cultured with MCF-7eGFP cells in parallel experiments, allowing direct comparison between cell lines on the growth outcome of MCF-7 cells. A spectrum of growth stimulation was observed (Fig. 1B). Surprisingly, both epithelial cells and fibroblasts were capable of stimulating growth, without being a universal feature of either cell type. Both of the non-human cell lines, the CV-1 (African Green Monkey) and MEF (mouse) significantly stimulated growth, indicating that the source of the signaling, that is, the specific cell type, does not alone dictate the permissiveness of the microenvironmental activity. Additionally, the unbiased approach of multiple, diverse co-cultures highlights the spectral effects on growth that may result both from the expression levels of specific growth factors and the combinatorial effects of multiple factors.

Transcriptional profile of estrogen-responsive genes

In models of hormonally responsive breast cancer, such as MCF-7 cells, growth is dependent on ERα signaling activation upon estrogen treatment. The growth observed in co-culture conditions lacking estrogen and its precursors suggest that ERα may be activated independent of ligand. ERα is a transcriptional regulator of a large set of genes in response to both ligand-dependent and -independent signaling. To test whether ERα was indeed activated, direct co-culture of MCF-7eGFP cells was performed with HS-5 cells, which induced the highest growth stimulation, and qRT-PCR analysis examined the changes in expression of ERα target genes in comparison to mono-culture. As the total RNA isolated included both MCF-7eGFP and HS-5 cell RNA, E-cadherin (*CDH1*) was used as an epithelial-specific reference gene to control for total MCF-7eGFP RNA in the sample. This analysis revealed a decrease in the gene encoding ERα (*ESR1*), which is consistent with a previously reported macrophage co-culture model.[46] Additionally, the transcriptional profile demonstrated an increase in expression of genes encoding the Progesterone Receptor (*PGR*), and pS2 (*TFF1*) (Fig. 2), which are dependent on ERα activation for expression. *ESR1*, *PGR*, and *TFF1* genes were not expressed in HS-5 cells, thus represent differential expression in the MCF-7eGFP cells only.

ERα protein dynamics in heterotypic cell culture

Clinically, ERα expression in breast cancers predicts the dependence of the tumor on estrogen for growth. ERα expression, however, is dynamic in response to activation, either in response to estrogen or ligand-independent signals. The gene expression profile of ERα target genes observed in MCF-7

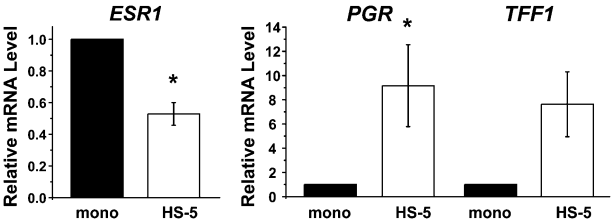

Fig. 2 Transcriptional profile of ERα target genes in response to co-culture. MCF-7eGFP cells in mono-culture or in direct co-culture with HS-5 cells in 6-well plates were harvested after 24 hours and RNA was isolated and reverse transcribed. Genes for ERα (*ESR1*), Progesterone Receptor (*PGR*), pS2 (*TFF1*), and E-cadherin (*CDH1*), which served as an MCF-7 cell-specific reference gene, were quantified by qRT-PCR. Error bars represent standard deviation of 4–5 independent experiments. Statistical significance is represented by * ($p < 0.05$ *versus* mono-culture).

co-cultures with bone marrow stromal cells indicates ERα activation. Thus, we would expect that target gene expression changes coincide with additional markers of activation, such as ERα protein down-regulation[20,21,25,47,48] and phosphorylation.[27] Microfluidic device culture and image analysis were optimized to assess ERα expression and signaling (Fig. 3A). Two specific devices are used here: the single microchannels and the two-channel compartmentalized device. Single microchannels directly co-culture cells in a total volume of 4 μL and were the predominant devices used here for their maximal sensitivity and high-throughput. The two-channel compartmentalized device, with a total volume of 40 μL, was used specifically to test the requirement of cell contact for the biological endpoints.

The ability to detect changes in protein levels by image analysis was validated using two methods. First, a dilution of MCF-7eGFP cells in single microchannels demonstrates that eGFP fluorescence intensity is linearly related to cell number, similar to growth assays (Fig. S2A, ESI†). Second, InSpeck microsphere beads with established relative intensity levels demonstrate that protein dynamics can also be detected to a 10^2 order of magnitude change with reasonable linearity (Fig. S2B, ESI†). The workflow for a typical protein quantification assay by image analysis is summarized in Fig. 3B. Proteins of interest are first labeled by standard immunofluorescence, and microscopy exposure settings maximizing the dynamic range are selected. Following background subtraction, image intensities were measured using ImageJ software. As with growth assays, the expression of eGFP provides an internal normalization and spatial identification of MCF-7eGFP cells, permitting measurement of target signal selectively from MCF-7 cells in heterotypic cultures.

To specifically model the interaction between breast cancer cells and the relevant stromal microenvironments of both primary and metastatic breast cancer, MCF-7 cells were co-cultured with bone marrow HS-5 cells, mammary fibroblast cell line RMF/EG, and lung fibroblast cell line MRC-5 for 24 hours in single microchannels, treated with or without 100 nM 17β-estradiol (E2) for the last 8 hours, then stained for ERα protein (representative images in Fig. 4A). Surprisingly, quantification of ERα protein levels detected a significant decrease

Published on 27 March 2013. Downloaded by University of Arizona on 29/09/2014 15:24:34.

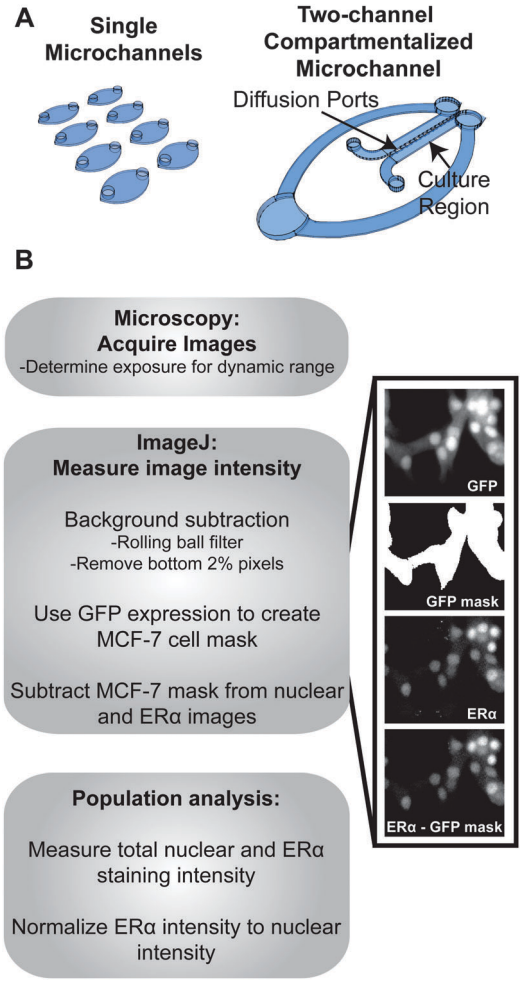

Fig. 3 Schematic of microfluidic devices and quantitative immunofluorescence procedure. (A) Microfluidic devices used were the single microchannels and two-channel compartmentalized microchannels. (B) Work flow of immunofluorescence image analysis at population level. Right panel depicts representative images from image analysis.

in all three co-culture conditions, as well as in response to the E2 positive control, relative to mono-cultured cells (Fig. 4B). An additional ERα-positive cell line, T47D, similarly down-regulated ERα protein levels upon co-culture with HS-5 cells, which was demonstrated in traditional macro-scale culture and Western blot (Fig. S3, ESI†). A further decrease in MCF-7 ERα levels upon treatment with E2 was seen only in co-culture with RMF/EG cells, although HS-5 cells displayed a similar trend. Treatment of MRC-5 co-cultures, however, resulted in an intermediate decrease between E2-treated MCF-7eGFP cells and MRC-5 co-culture. This could suggest that the co-cultures differ in the signaling pathways used to activate ERα, as signaling from MRC-5 cells appears to preclude estrogen-dependent activation of the receptor, whereas HS-5 and RMF/EG signaling appears to overlap with estrogen signaling. In the following experiments, HS-5 cells were more closely examined as the most robust model for inducing ERα, as it is an ideal model for looking more specifically at ERα signaling and a useful reference point for experiments that expand on the co-culture models examined.

All co-cultures were conducted in media stripped of all steroid molecules, including precursors of estradiol to avoid estrogen synthesis. To test the possibility of ligand-dependent activation further, MCF-7 co-cultures with HS-5 were treated with the competitive inhibitor for estrogen binding, Tamoxifen (OHT), which did not prevent the down-regulation of ERα in HS-5 co-cultures (Fig. S4A, ESI†). Additionally, treatment with the aromatase inhibitor Anastrozole (Ana), which blocks the enzyme responsible for converting androgens into estrogens, did not recover ERα expression in HS-5 co-cultures (Fig. S4B, ESI†), again, indicating that estrogens synthesized by the aromatase-expressing HS-5 cells are not stimulating the ERα pathway.

HS-5 and MDA-MB-231 cells demonstrated high growth stimulation and ERα down-regulation, and were therefore selected as sensitive models for further analysis. The two-channel compartmentalized device, allows diffusion-based communication between two cell culture regions through diffusion ports measuring 10 μm high and 100 μm wide. The utility of this device is analogous to commercially available membrane inserts, and further benefits from the ability to image both culture regions in the same plane with enhanced sensitivity.[34] Co-culture in compartmentalized microfluidic devices demonstrates that down-regulation of ERα protein does not require heterotypic cell–cell contact between MCF-7eGFP cells and MDA-MB-231 cells, and must occur through soluble factors (Fig. 4C). After 24 hours of co-culture with HS-5 cells in single microchannels, immunofluorescence image analysis of MCF-7eGFP cells detects an increase in the level of phosphorylation of ERα at Serine-118 (S118), a site essential for full activity of the receptor[26,49] (Fig. 4D). Note that the levels of phosphorylated S118 are not normalized to total ERα protein, and thus reflect a large shift in the proportion of phosphorylated ERα protein since the total ERα levels are decreased at this time point. The total ERα antibody used in immunofluorescence staining does not discriminate between unphosphorylated and phosphorylated ERα.[50] ERα down-regulation was hereafter selected as a surrogate marker of ERα activation in following co-culture assays based on the transcriptional profile of ERα activation and the presence of phosphorylation consistent with receptor activation.

Single-cell analysis to examine intra-population ERα distribution

Using single-cell analysis, protein levels can be quantified per cell, providing information on the distribution of protein expression within a population. Following measurement of ERα staining within the boundaries created by nuclear staining, a histogram of ERα staining intensity describes the distribution of ERα protein within a population (Fig. 5). To account for variations in MCF-7 cell number in each culture condition, the frequency of nuclei expressing each ERα expression level was normalized to the total number of particles in each condition, and therefore the area under each raw curve is equal to one. The height and width of the histogram therefore describe the degree of heterogeneity in expression, where a taller, narrower peak describes more homogenous expression in the population. Surprisingly, we found that mono-cultured MCF-7 cells

 This journal is © The Royal Society of Chemistry 2013

Published on 27 March 2013. Downloaded by University of Arizona on 29/09/2014 15:24:34.

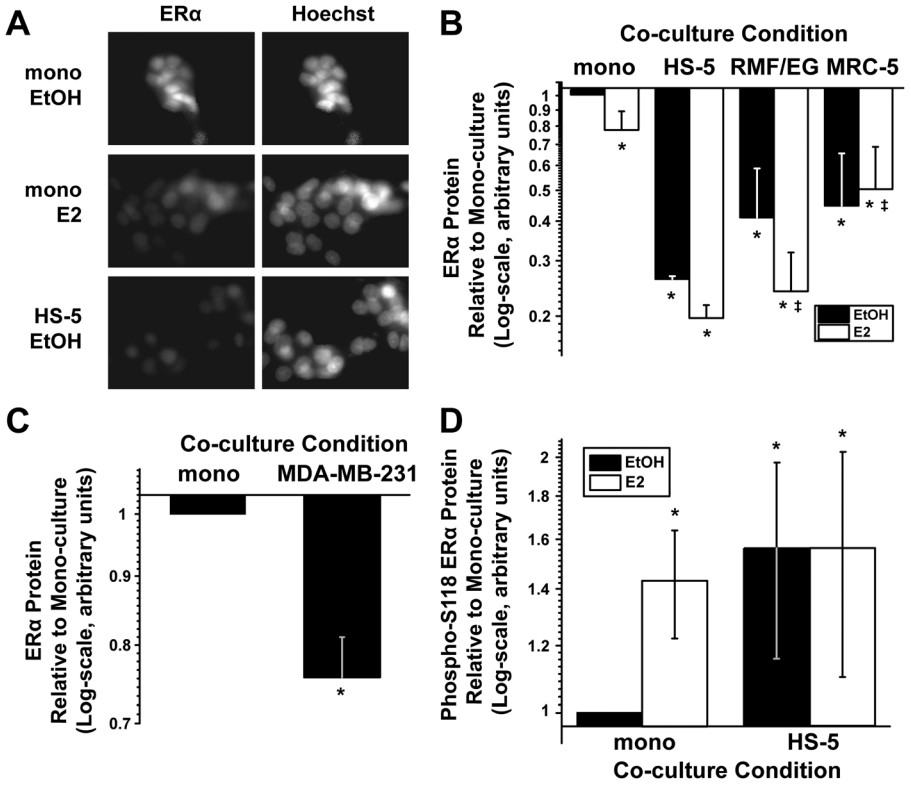

Fig. 4 ERα protein expression and phosphorylation in co-culture. (A) Representative immunofluorescence images of ERα and Hoechst (nuclear) staining from single microchannels. (B) Quantified ERα immunofluorescence relative to mono-cultured, vehicle-treated MCF-7eGFP cells. MCF-7eGFP cells were cultured alone (mono) or with bone marrow stromal cells (HS-5), human mammary fibroblasts (RMF/EG), or lung fibroblasts (MRC-5) for 24 hours in single microchannels and treated for the last 8 hours with 100 nM 17β-estradiol (E2) or vehicle (EtOH). In each of three experiments, 5–10 internal replicates were performed. (C) MCF-7eGFP cells cultured with or without MDA-MB-231 cells in two-channel compartmentalized microfluidic devices for 24 hours were stained for ERα protein and analyzed as in B. (D) MCF-7eGFP cells were cultured with or without HS-5 cells for 20 hours in single microchannels and treated with 100 nM 17β-estradiol (E2) or vehicle (EtOH) for the last 30 minutes. Staining of ERα Serine-118 phosphorylation in MCF-7eGFP cells was quantified by immunofluorescence image analysis as in Fig. 3B. The means of each experiment were averaged, and error bars represent standard error of the mean between the three independent experiments. Statistical significance is represented by symbols: * = *versus* mono-culture, vehicle-treated MCF-7eGFP ($p < 0.05$), ‡ = *versus* respective vehicle-treated co-culture ($p < 0.05$).

had some degree of heterogeneity in ERα protein expression per cell, despite the clonal origin of cell lines. Upon co-culture with HS-5 cells, the ERα protein levels not only decrease, but become more homogenous within the co-cultured population. Similar trends were observed with CV-1 cells (data not shown), which also demonstrated a high growth stimulation of MCF-7 cells.

Relating ERα protein levels to growth in co-culture

While the cell panel did not reveal patterns of microenvironmental activity based on cell type or organ origin on growth of MCF-7eGFP in co-culture, combining ERα protein dynamics as a measure of ERα activity with growth outcome infers the role of ERα signaling in growth stimulation from the microenvironmental activity. ERα protein in MCF-7eGFP cells co-cultured with the cell panel in single microchannel devices was quantified by immunofluorescence image analysis. As in the growth data, a spectrum of changes in ERα protein levels was observed with no clear pattern based on cell type or original organ site (Fig. 6A). However, when ERα levels were plotted against their paired growth effect, a significant correlation was observed (Fig. 6B). Intriguingly, two data points, representing HS-5 and MEF co-cultures, lie farthest above the line of best fit. Additional axes were superimposed on the plot to distinguish samples that had significant changes in growth (horizontal axis) and/or ERα down-regulation (vertical axis). These axes form four quadrants that lead to distinct patterns of growth. Those samples without growth or ERα changes suggest that the micro-environmental activity of these co-culture pairs is inert in terms of these parameters. In the upper-left quadrant, ERα down-regulation correlates with growth stimulation in the MCF-7 cells, which would lead to the hypothesis that in these co-cultures the microenvironmental activity promotes ligand-independent activation of the receptor, which is driving the proliferation. Interestingly, one co-culture falls in the upper-right quadrant, suggesting that MEF cells may stimulate the growth of MCF-7 cells by an alternative, ERα-independent pathway. Encouragingly, no cell lines lie in the quadrant that would suggest that ERα activity is not related to growth.

Discussion

Clinically, ERα expression in tumor cells is used as a predictive measure of the effectiveness of hormonal therapies that target

Published on 27 March 2013. Downloaded by University of Arizona on 29/09/2014 15:24:34.

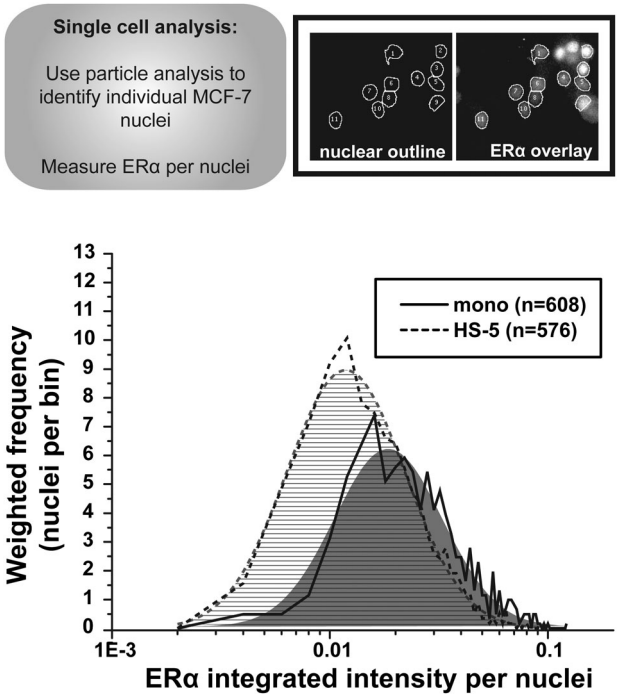

Fig. 5 Population distribution of ERα protein in mono-cultured and HS-5 co-cultured MCF-7eGFP cells from single microchannels. Single-cell analysis of immunofluorescence images was performed to identify individual MCF-7eGFP nuclei as individual particles and ERα intensity per nuclei was measured as described in the top panel. Four representative image views per condition were processed, encompassing a total of 400–700 cells per condition, where the specific number of cells (*n*) for each condition is specified in the histogram in the bottom panel. To allow direct comparison between conditions for determination of heterogeneity, the frequencies of events per bin (*i.e.* image intensity interval) were weighted by *n* for the respective condition, resulting in an area under the curve of 1. The raw curves were then modeled using Log-normal peak fits, shown as shaded curves.

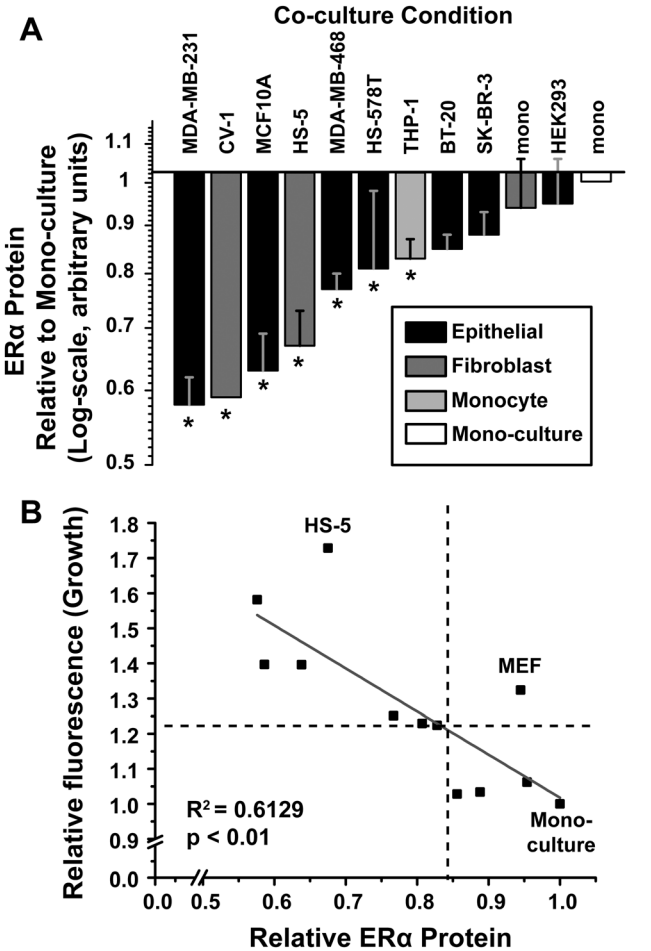

Fig. 6 ERα protein quantification in MCF-7eGFP cell panel co-culture. (A) MCF-7eGFP cells were co-cultured with the cell panel described in Fig. 1 for 24 hours in single microchannels, and stained for ERα protein. Immunofluorescence image analysis was performed as in Fig. 3B. Statistical significance is represented by * ($p < 0.05$ *versus* mono-culture). (B) ERα protein level was plotted against its respective fold growth in Fig. 1B. Spearman's correlation test was used to determine correlation between the two parameters, and the R^2 value is derived from the linear best-fit line. Quadrants were superimposed by creating axes between significant and non-significant differences in growth and ERα down-regulation.

and inactivate ERα. In contrast to early stage breast cancer, metastatic tumors exist in unique non-native environments such as bone, liver, pleura, and brain. These unnatural contexts generate specific microenvironments that interact with tumor cells *via* complex and varying signaling events, making it challenging to assess cumulative effects. Here, we show a correlation between the degree of growth stimulation and ERα down-regulation upon co-culture with a cell line array, which has a number of novel implications. While the outcomes of ERα protein down-regulation and growth stimulation are well known responses to ERα activation, the surprisingly linear relationship between these two outcomes in response to diverse signaling inputs has not been realized previously. This finding implies that dynamic measure of ERα protein levels may have utility as a sensor to predict how cell-extrinsic signaling modulates growth of hormonally-responsive breast cancer cells. Further, the data indicate that the microenvironmental activity may initiate growth through ligand-independent, and potentially SERM-refractory, mechanisms. Thus, the expansion of ERα from a tumor biomarker to a dynamic microenvironment biosensor capitalizes on our current knowledge and incorporates a functional measure of microenvironmental activity, which could better inform therapy decisions.

The novel approaches utilized were instrumental in allowing detection of the correlation between ERα and growth. The small scale of microfluidic culture enabled high-throughput operation amenable to the cell culture array, allowing a number of replicates and conditions with fewer resources than traditional culture scales. The use of image analysis in measuring protein levels aids in the downstream detection of endpoints with distinct advantages over other approaches. In comparison to traditional approaches such as Western blots, image analysis is more scalable to high-throughput assays without significantly adding to the workload and time to analysis. The spatial information provided by image analysis provides an additional level of information to incorporate into analysis. Here we have described how this aids in selective detection of the target protein using cell markers and masking techniques and the ability to measure protein at the cellular level. Additional utilities

 This journal is © The Royal Society of Chemistry 2013

Published on 27 March 2013. Downloaded by University of Arizona on 29/09/2014 15:24:34.

of the spatial parameter may include detection of gradient effects within a population in response to a given signal and co-localization of additional proteins, such as proliferation markers, to a single cell. Ultimately, the combination of the microfluidic system with canonical model of hormonally responsive breast cancer, MCF-7 cells, creates an assay of the microenvironmental activity of the breast cancer cellular context.

Closer examination of the ERα *vs.* growth plot reveals that two heterotypic cell culture conditions appear to lie farther from the general trend. Interestingly, both conditions demonstrate disproportionate growth stimulation when compared to the level of ERα down-regulation, consistent with an ERα-independent mode of growth. This could occur through stimulation of alternative signaling pathways for growth, bypassing the requirement for ERα. These outliers may therefore represent a microenvironmental activity that is hormone therapy refractive. *In vitro* testing is underway to determine whether ERα is necessary for growth stimulated by microenvironmental activity and if ERα dynamics predict hormone therapy response. Our growth and ERα protein assays are ideal for studies using human primary cells,[51,52] in which the microenvironmental activity surrounding the tumor could be sampled in co-culture with MCF-7 cells, serving as biomarker cells for ERα activation. The results presented here serve as a proof-of-principle for the feasibility of such assays. Such an approach may be linked to clinical responses in the future to test predictions of therapy response.

Acknowledgements

We thank McArdle Laboratories for Cancer Research for support on this project. We also thank the UW Carbone Comprehensive Cancer Center (UWCCC) for use of its shared services to complete this research. We thank Drs. Daniel Loeb and Andreas Friedl for providing reagents and cells. We thank Dr. Edmond Young on his guidance in single-cell analysis. This work was supported by NIH grants CA159578 (to E.T.A.) and CA137673 (to E.T.A. and D.J.B.) and T32 CA009135 (to J.D.L. and G.L.P.).

References

1 C. M. Nelson and M. J. Bissell, *Annu. Rev. Cell Dev. Biol.*, 2006, **22**, 287–309.
2 F. Moinfar, Y. G. Man, L. Arnould, G. L. Bratthauer, M. Ratschek and F. A. Tavassoli, *Cancer Res.*, 2000, **60**, 2562–2566.
3 D. Hanahan and R. A. Weinberg, *Cell*, 2011, **144**, 646–674.
4 M. J. Bissell and W. C. Hines, *Nat. Med.*, 2011, **17**, 320–329.
5 J. L. Camps, S. M. Chang, T. C. Hsu, M. R. Freeman, S. J. Hong, H. E. Zhau, A. C. von Eschenbach and L. W. Chung, *Proc. Natl. Acad. Sci. U. S. A.*, 1990, **87**, 75–79.
6 C. E. van Roozendaal, B. van Ooijen, J. G. Klijn, C. Claassen, A. M. Eggermont, S. C. Henzen-Logmans and J. A. Foekens, *Br. J. Cancer*, 1992, **65**, 77–81.
7 H. L. Neville-Webbe, N. A. Cross, C. L. Eaton, R. Nyambo, C. A. Evans, R. E. Coleman and I. Holen, *Breast Cancer Res. Treat.*, 2004, **86**, 269–279.
8 Q. Chen, X. H. Zhang and J. Massague, *Cancer Cell*, 2011, **20**, 538–549.
9 A. E. Karnoub, A. B. Dash, A. P. Vo, A. Sullivan, M. W. Brooks, G. W. Bell, A. L. Richardson, K. Polyak, R. Tubo and R. A. Weinberg, *Nature*, 2007, **449**, 557–563.
10 K. E. Corcoran, K. A. Trzaska, H. Fernandes, M. Bryan, M. Taborga, V. Srinivas, K. Packman, P. S. Patel and P. Rameshwar, *PLoS One*, 2008, **3**, e2563.
11 A. Orimo, P. B. Gupta, D. C. Sgroi, F. Arenzana-Seisdedos, T. Delaunay, R. Naeem, V. J. Carey, A. L. Richardson and R. A. Weinberg, *Cell*, 2005, **121**, 335–348.
12 M. Bauer, G. Su, D. J. Beebe and A. Friedl, *Integr. Biol.*, 2010, **2**, 371–378.
13 L. J. Hofland, B. van der Burg, C. H. van Eijck, D. M. Sprij, P. M. van Koetsveld and S. W. Lamberts, *Int. J. Cancer*, 1995, **60**, 93–99.
14 P. Briand, B. K. Lundholt, J. Skouv and A. E. Lykkesfeldt, *Mol. Cell. Endocrinol.*, 1999, **153**, 1–9.
15 S. Loi, C. Sotiriou, B. Haibe-Kains, F. Lallemand, N. M. Conus, M. J. Piccart, T. P. Speed and G. A. McArthur, *BMC Med. Genomics*, 2009, **2**, 37.
16 W. Kung, F. David, H. Langen, K. A. Weyer, E. J. Schlaeger, H. W. Lahm, E. Silber, H. Mueller and U. Eppenberger, *Biochem. Biophys. Res. Commun.*, 1994, **202**, 1357–1365.
17 A. J. Stewart, M. D. Johnson, F. E. May and B. R. Westley, *J. Biol. Chem.*, 1990, **265**, 21172–21178.
18 M. Bartucci, C. Morelli, L. Mauro, S. Ando and E. Surmacz, *Cancer Res.*, 2001, **61**, 6747–6754.
19 E. M. Fox, T. W. Miller, J. M. Balko, M. G. Kuba, V. Sanchez, R. A. Smith, S. Liu, A. M. Gonzalez-Angulo, G. B. Mills, F. Ye, Y. Shyr, H. C. Manning, E. Buck and C. L. Arteaga, *Cancer Res.*, 2011, **71**, 6773–6784.
20 L. D. Read, G. L. Greene and B. S. Katzenellenbogen, *Mol. Endocrinol.*, 1989, **3**, 295–304.
21 J. J. Pink and V. C. Jordan, *Cancer Res.*, 1996, **56**, 2321–2330.
22 A. M. Nardulli, G. L. Greene, B. W. O'Malley and B. S. Katzenellenbogen, *Endocrinology*, 1988, **122**, 935–944.
23 J. R. Schultz, L. N. Petz and A. M. Nardulli, *Mol. Cell. Endocrinol.*, 2003, **201**, 165–175.
24 J. Kim, L. N. Petz, Y. S. Ziegler, J. R. Wood, S. J. Potthoff and A. M. Nardulli, *J. Steroid Biochem. Mol. Biol.*, 2000, **74**, 157–168.
25 E. T. Alarid, N. Bakopoulos and N. Solodin, *Mol. Endocrinol.*, 1999, **13**, 1522–1534.
26 P. Le Goff, M. M. Montano, D. J. Schodin and B. S. Katzenellenbogen, *J. Biol. Chem.*, 1994, **269**, 4458–4466.
27 S. Ali, D. Metzger, J. M. Bornert and P. Chambon, *EMBO J.*, 1993, **12**, 1153–1160.
28 G. Bunone, P. A. Briand, R. J. Miksicek and D. Picard, *EMBO J.*, 1996, **15**, 2174–2183.
29 C. L. Smith, *Biol. Reprod.*, 1998, **58**, 627–632.
30 R. I. Nicholson, I. R. Hutcheson, D. Britton, J. M. Knowlden, H. E. Jones, M. E. Harper, S. E. Hiscox, D. Barrow and J. M. Gee, *J. Steroid Biochem. Mol. Biol.*, 2005, **93**, 257–262.
31 S. Baron, A. Escande, G. Alberola, K. Bystricky, P. Balaguer and H. Richard-Foy, *J. Biol. Chem.*, 2007, **282**, 11732–11741.

Published on 27 March 2013. Downloaded by University of Arizona on 29/09/2014 15:24:34.

32 K. Sauve, J. Lepage, M. Sanchez, N. Heveker and A. Tremblay, *Cancer Res.*, 2009, **69**, 5793–5800.
33 G. M. Walker and D. J. Beebe, *Lab Chip*, 2002, **2**, 131–134.
34 M. Domenech, H. Yu, J. Warrick, N. M. Badders, I. Meyvantsson, C. M. Alexander and D. J. Beebe, *Integr. Biol.*, 2009, **1**, 267.
35 G. M. Walker, H. C. Zeringue and D. J. Beebe, *Lab Chip*, 2004, **4**, 91–97.
36 E. W. Young and D. J. Beebe, *Chem. Soc. Rev.*, 2010, **39**, 1036–1048.
37 I. Meyvantsson and D. J. Beebe, *Annu. Rev. Anal. Chem.*, 2008, **1**, 423–449.
38 C. Ortiz De Solorzano, S. Costes, D. E. Callahan, B. Parvin and M. H. Barcellos-Hoff, *Microsc. Res. Tech.*, 2002, **59**, 119–127.
39 J. P. Puccinelli, X. Su and D. J. Beebe, *JALA*, 2010, **15**, 25–32.
40 K. J. Regehr, M. Domenech, J. T. Koepsel, K. C. Carver, S. J. Ellison-Zelski, W. L. Murphy, L. A. Schuler, E. T. Alarid and D. J. Beebe, *Lab Chip*, 2009, **9**, 2132.
41 N. R. Drinkwater and C. Denniston, *Statistical Problems in Genetics and Molecular Biology*, Createspace, 2011.
42 C. C. Valley, N. M. Solodin, G. L. Powers, S. J. Ellison and E. T. Alarid, *J. Mol. Endocrinol.*, 2008, **40**, 23–34.
43 K. J. Livak and T. D. Schmittgen, *Methods*, 2001, **25**, 402–408.
44 J. S. Yuan, A. Reed, F. Chen and C. N. Stewart, Jr., *BMC Bioinf.*, 2006, **7**, 85.
45 M. D. Abramoff, P. J. Magelhaes and S. J. Ram, *Biophotonics Int.*, 2004, **11**, 36–42.
46 F. Stossi, Z. Madak-Erdogan and B. S. Katzenellenbogen, *Oncogene*, 2012, **31**, 1825–1834.
47 Z. Nawaz, D. M. Lonard, A. P. Dennis, C. L. Smith and B. W. O'Malley, *Proc. Natl. Acad. Sci. U. S. A.*, 1999, **96**, 1858–1862.
48 A. El Khissiin and G. Leclercq, *FEBS Lett.*, 1999, **448**, 160–166.
49 P. B. Joel, A. M. Traish and D. A. Lannigan, *J. Biol. Chem.*, 1998, **273**, 13317–13323.
50 M. H. Al-Dhaheri and B. G. Rowan, *Nucl. Recept. Signaling*, 2006, **4**, e007.
51 H. Yu, C. M. Alexander and D. J. Beebe, *Lab Chip*, 2007, **7**, 388–391.
52 E. W. Young, C. Pak, B. S. Kahl, D. T. Yang, N. S. Callander, S. Miyamoto and D. J. Beebe, *Blood*, 2012, **119**, e76–e85.

 This journal is © The Royal Society of Chemistry 2013